Graph-Theoretical Approach to Multiple Scattering by Polygonal Cylinders

Danilo Erricolo, Piergiorgio L.E. Uslenghi

Department of Electrical Engineering and Computer Science, University of Illinois at Chicago
1120 SEO (MC 154), 851 South Morgan Street, Chicago, IL 60607-7053 USA
Tel. +1-312-996-5771, Fax +1-312-413-0024, E-mail derricol@eecs.uic.edu

Abstract— **The electromagnetic scattering of a cylindrical wave by a group of polygonal cylinders is studied in the two-dimensional case using ray tracing methods. All ray trajectories connecting the source to the observation point can be computed up to any arbitrary order. The polygonal cylinders are electrically characterized by a surface impedance and they can be either concave or convex.**

I. Introduction

The problem of the electromagnetic scattering of a cylindrical wave incident on a group of two-dimensional polygonal cylinders is considered. The goal of this study is the evaluation of the field intensity at an arbitrary observation point, while accounting for the interaction of the cylindrical wave with the polygonal obstacles. The study is carried out using ray tracing methods, which implies the determination of all the trajectories connecting the source point to the observation point. The approach taken consists of:

- Preprocessing the information related to the position of the polygonal cylinders. This operation is carried out to establish the "local" visibility that each polygon has towards its neighbors.
- The construction of an overall visibility graph using the results found in the previous step.
- The extraction of the ray trajectories connecting the source point to the observation point by means of a traversal algorithm that is applied to the overall visibility graph.

For each ray trajectory, it must be verified that both geometrical optics (i.e., reflection law) and geometrical theory of diffraction (i.e., edge diffraction law) are fulfilled. Then the field strength at the observation point is computed by coherent superposition of the field strength associated with each ray trajectory. The field intensity of each ray trajectory is calculated by introducing the proper reflection and diffraction coefficients along the path. The electromagnetic properties of the polygonal cylinders are given in terms of surface impedance, which makes this study quite flexible in terms of the variety of situations that can be represented. Finally, the algorithm is implemented in C++ language to take full advantage of the methodologies offered by object-oriented programming.

II. The Method

Free space propagation and reflection are easily treated with ordinary ray tracing methods. Diffraction cannot be studied using an ordinary ray tracing approach because of the law of edge diffraction according to which a ray incident on an edge creates a whole cone of diffracted rays. Therefore, an inverse method is used to avoid the problem of dealing with a cone of an infinite number of diffracted rays. The idea is to consider two points, the source and the observation, and to connect them with all the trajectories that it is possible to draw according with the constraints imposed by the environment. The environment is a plane where objects with the shape of polygons are present. The polygons can be concave or convex and both their faces and vertices will be referred to as the scattering elements of the environment. Rays that propagate from the source to the observation point interact with the environment at the scattering elements. The interactions at the scattering elements are either reflections or diffractions. For a given ray trajectory, the number of interactions at the scattering elements determines the order of the ray. Therefore, a direct ray from source to observation is a zero order path, whereas a ray that undergoes either one reflection or one diffraction during its propagation will be referred to as a first order path. The algorithm that will be presented can compute the trajectories under the assumption that a given path must not pass twice through the same point. The algorithm determines the trajectories starting from order zero up to a specified order. The first order trajectory is computed using the following steps:

1. All scattering elements that are visible from the source (i.e. all elements that have a line of sight with the source) are determined and collected together in what will be referred to as the visibility list of the source.

2. Each element of the visibility list that has a line of sight with the observation point is selected to become part of a candidate trajectory.
3. The candidate trajectory is composed of the source, the scattering element, and the observation point. If the scattering element is a vertex, where a diffraction occurs, then the trajectory passing through the scattering element is a physical trajectory. However, if the scattering element is a segment, one has to establish whether the angles of incidence and reflection satisfy the reflection law.

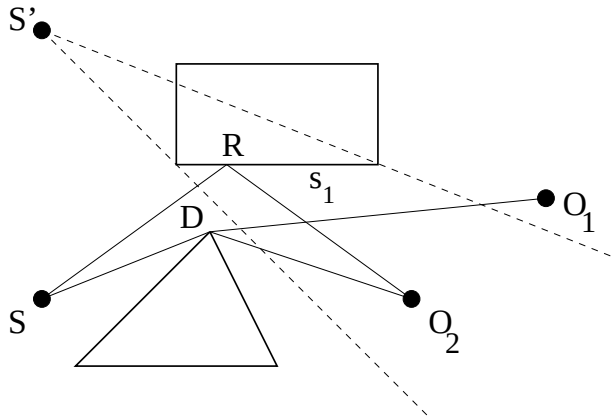

Fig. 1. Candidate first order trajectories

The previous concepts are better explained referring to Figure 1. The source S has visibility with many scattering elements and, in particular, with segment s_1. Because s_1 has a line of sight with O_1, the algorithm considers the candidate trajectory:

$$S \rightarrow s_1 \rightarrow O_1 \ . \tag{1}$$

However, no point on s_1 satisfies the reflection law and the trajectory (1) is discarded. Point O_2 also has a line of sight with s_1 and, in this case, the candidate trajectory:

$$S \rightarrow s_1 \rightarrow O_2 \tag{2}$$

satisfies the reflection law with a reflection at point R to produce the actual physical trajectory:

$$S \rightarrow R \rightarrow O_2 \ . \tag{3}$$

The source point S has also visibility towards D, which, in turn, has visibility towards O_1 andO_2. Because D is a diffraction point and this is a plane case, all diffraction angles are possible and the two trajectories:

$$S \rightarrow D \rightarrow O_1 \tag{4}$$
$$S \rightarrow D \rightarrow O_2 \tag{5}$$

are physical.

III. Determination of the visibility

One of the most difficult tasks to solve in this problem is the determination of the visibility in an environment with a potentially large number of objects. A statistics of ray tracing applications shows that, in order to render images where thousands of objects are present, more than 95% of the time is spent performing intersection calculations between rays and objects [1], if an exhaustive approach is taken. An exhaustive implementation is prohibitive and before implementing any ray tracing algorithm it is necessary to become acquainted with acceleration techniques [2]. The first step to accelerate intersection computations consists of enclosing each polygon into a rectangular bounding box. Bounding boxes are approximate convex hulls having the property that if a ray does not pierce the bounding box, the ray cannot intersect the polygon inside the box. Bounding boxes are advantageous because it is easier to compute an intersection with the bounding box instead of computing an intersection with the actual polygon. If the ray pierces the bounding box, then one needs to compute the intersection with the polygon too and, in this case, the presence of the bounding box increases the number of intersection calculations, but, on average, the computations for intersection are faster. Bounding boxes do not reduce the number of objects to intersect, but make those intersection computations faster. A further improvement consists of creating a hierarchical structure of bounding boxes that contain groups of bounding boxes. In this way, only the bounding boxes that are pierced by the rays are considered, therefore greatly reducing the number of intersection calculations. Figure 2 shows three polygons,

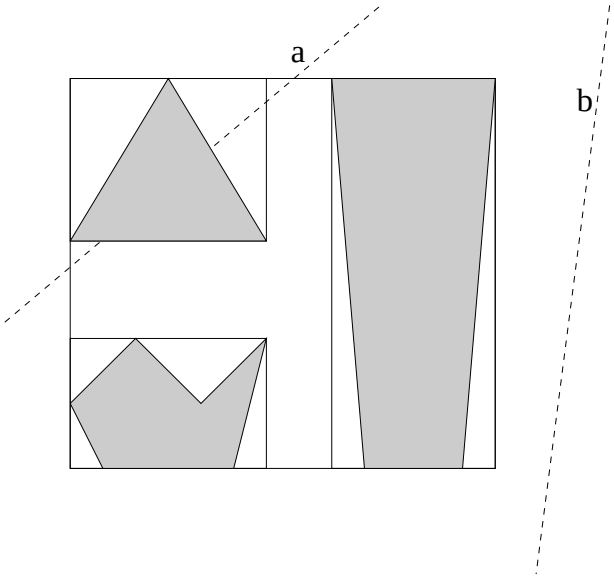

Fig. 2. Polygons and their bounding boxes

each one of them contained in its own bounding box and the overall bounding box. Ray b does not intersect the larger bounding box, therefore the computations for a possible intersection with the smaller bounding boxes are avoided. Ray a does pierce the large bounding box, hence the intersection computations have to be performed in this case. The authors have chosen to follow the implementation of Wilt [3] for the bounding

volume hierarchy proposed by Goldsmith and Salmon [4]. A final improvement consists of introducing the so

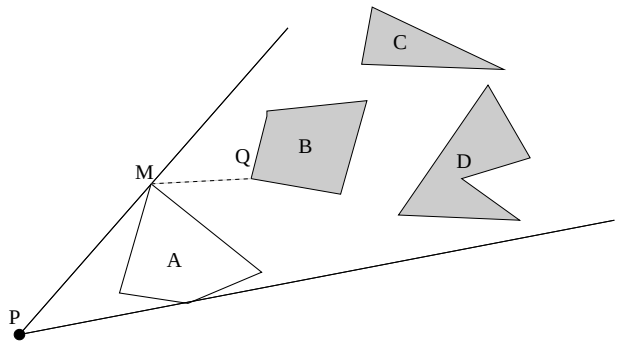

Fig. 3. Painter's algorithm

called painter's algorithm that simply consists of keeping track of the objects that have a line of sight with the point of view and neglecting those that are shadowed by the closest ones. Figure 3 shows that the presence of object A shadows objects B, C, and D. Therefore, the last three objects do not need to be further investigated because object A is the only object visible from P and there is no direct trajectory going from P to any of the objects B, C, and D. However, a trajectory from P to Q is built in two steps: using the visibility from P one gets to M and, from the visibility from M one finally reaches Q.

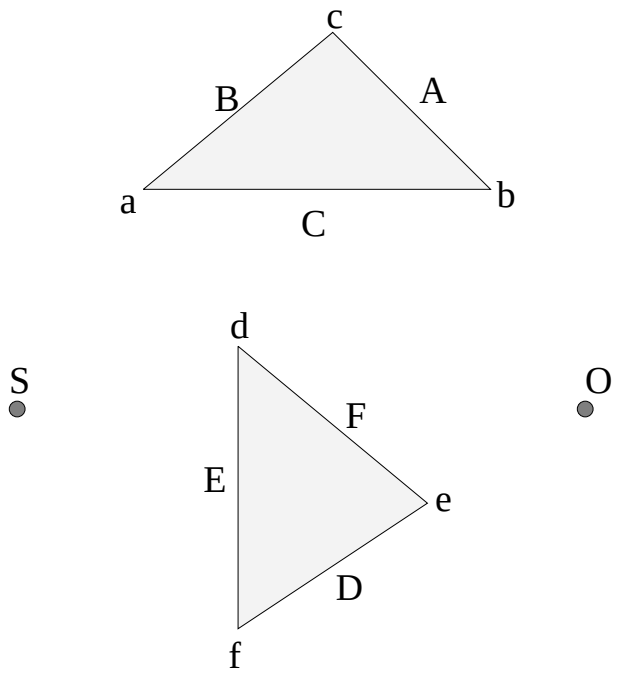

Fig. 4. Sample environment

IV. The graph theoretical model

For the environment shown in Figure 4 one could draw a graph that collects all the visibility information obtained for each scattering element. The information is presented in Figure 5 and it represents a collection of elements that have a line of sight among each other. The process of the determination of the trajectories outlined in Section II can be thought of as the extraction of the paths of Figure 5 that connect S with O. Because of the reasons previously explained, all paths containing at least one reflection need to be checked to assess whether they satisfy the reflection law.

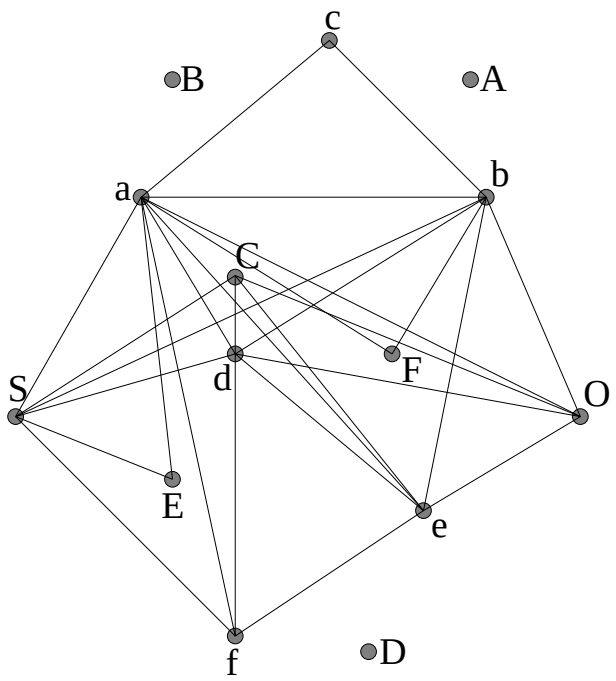

Fig. 5. Visibility graph

V. Mathematical Models

There are two mechanisms that change the direction of propagation of a ray: reflection and diffraction. Reflections are accounted for by using the reflection coefficient for an impedance plane:

$$R = \frac{\sin\phi_0 - \sin\theta}{\sin\phi_0 + \sin\theta} \tag{6}$$

where ϕ_0 is the angle between the surface and the incidence direction and θ is a parameter related to the normalized surface impedance η by:

$$\sin\theta = \begin{cases} 1/\eta & \text{E polarization} \\ \eta & \text{H polarization .} \end{cases} \tag{7}$$

Diffractions from impedance wedges are computed using the following coefficient [5], [6],

$$D(\phi,\phi',\theta_+,\theta_-) = -\frac{e^{-j\pi/4}}{2n\sqrt{2\pi k_0}}$$
$$\{\ \frac{\Psi(\frac{n\pi}{2}-\pi-\phi)}{\Psi(\frac{n\pi}{2}-\phi')}\cot\frac{\pi+(\phi-\phi')}{2n}F(k_0La_i^-)$$

$$+\frac{\Psi(\frac{n\pi}{2}+\pi-\phi)}{\Psi(\frac{n\pi}{2}-\phi')}\cot\frac{\pi-(\phi-\phi')}{2n}F(k_0La_i^-)$$
$$+R_\perp^-\frac{\Psi(\frac{n\pi}{2}-\pi-\phi)}{\Psi(-\frac{3n\pi}{2}+\phi')}\cot\frac{\pi+(\phi+\phi')}{2n}F(k_0La_r^+)$$
$$+R_\perp^+\frac{\Psi(\frac{n\pi}{2}+\pi-\phi)}{\Psi(\frac{n\pi}{2}+\phi')}\cot\frac{\pi-(\phi+\phi')}{2n}F(k_0La_i^+)\Bigg\}\ , \quad (8)$$

which applies to both E polarization and H polarization depending on the value of θ, chosen according to (7). Strictly speaking, this formula applies to a plane wave perpendicularly incident on the edge of a wedge with external angle factor n (i.e., $n\pi$ is the external angle in radians); however we use it for cylindrical wave incidence assuming that the incoming wave is locally plane when it reaches the edge. This assumption is approximately satisfied whenever the number of wavelengths between the source and the diffracting edge is large at the frequencies normally used for cellular communications inside cities. Therefore, L in (8) is the UTD distance parameter for cylindrical wave incidence, which is given by:

$$L=\frac{\rho\rho'}{\rho+\rho'}\ . \quad (9)$$

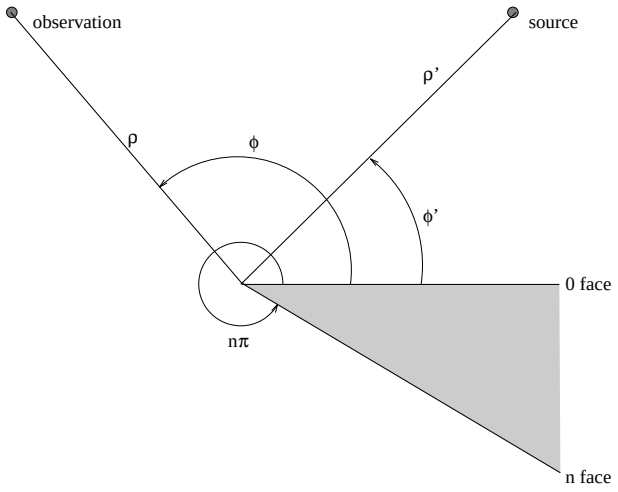

Fig. 6. Geometry for single impedance wedge diffraction

In (8), θ_+ and θ_- represent the value of θ for the 0-face and the n-face of the wedge, respectively; ϕ and ϕ' are the observation and incidence angles referred to the zero face; k_0 is the wavenumber. The symbols $R_\perp^+$ and $R_\perp^-$ are the reflection coefficients for the 0 face and the n face of the wedge, respectively, in the case of E polarization. Their expressions are:

$$R_\perp^+=\frac{\sin\phi_0-\sin\theta_+}{\sin\phi_0+\sin\theta_+}\ , \quad (10)$$

$$R_\perp^-=\frac{\sin n\pi-\phi_0-\sin\theta_-}{\sin n\pi-\phi_0+\sin\theta_-}\ . \quad (11)$$

F is the Kouyoumjian-Pathak transition function [7]:

$$F(X)=2j\sqrt{X}e^{jX}\int_{\sqrt{X}}^{\infty}e^{-j\tau^2}d\tau \quad (12)$$

and the functions $a_i^\pm$ and a_r^+ are:

$$a_i^\pm\approx 2\cos^2\frac{\phi\pm\phi_0}{2}\ , \quad (13)$$

$$a_r^+\approx 2\cos^2\frac{2n\pi-(\phi+\phi_0)}{2}\ . \quad (14)$$

The ratios which appear in front of the cotangent in (8) are expressed in terms of the Maliuzhinets function $\psi_{n\pi/2}$ as [8]:

$$\Psi(\alpha)=\psi_{n\pi/2}(\alpha+n\pi/2+\theta_+-\frac{\pi}{2})\cdot\psi_{n\pi/2}(\alpha+n\pi/2-\theta_++\frac{\pi}{2})\cdot\psi_{n\pi/2}(\alpha-n\pi/2+\theta_--\frac{\pi}{2})\cdot\psi_{n\pi/2}(\alpha-n\pi/2-\theta_-+\frac{\pi}{2}) \quad (15)$$

where $n\pi/2$ represents half of the external wedge angle. In the particular case of a perfect electrical conductor, the diffraction coefficient (8) reduces to the expression originally given by Kouyoumjian and Pathak [7]:

$$D_1=-\frac{e^{-j\pi/4}}{2n\sqrt{2\pi\beta}}\cot\left[\frac{\pi+(\phi-\phi')}{2n}\right]F[\beta La^+(\phi-\phi')]-\frac{e^{-j\pi/4}}{2n\sqrt{2\pi\beta}}\cot\left[\frac{\pi-(\phi-\phi')}{2n}\right]F[\beta La^-(\phi-\phi')]\pm\Bigg\{-\frac{e^{-j\pi/4}}{2n\sqrt{2\pi\beta}}\cot\left[\frac{\pi+(\phi+\phi')}{2n}\right]F[\beta La^+(\phi+\phi')]-\frac{e^{-j\pi/4}}{2n\sqrt{2\pi\beta}}\cot\left[\frac{\pi-(\phi+\phi')}{2n}\right]F[\beta La^-(\phi+\phi')]\Bigg\} \quad (16)$$

where the upper sign applies for hard polarization and the lower sign for soft polarization. In (16) L is the distance parameter (9) and the functions $a^\pm$ are given by:

$$a^\pm(X)=1+\cos(X-2n\pi N^\pm) \quad (17)$$

where $N^\pm$ are the integers which most closely satisfy:

$$\begin{array}{ll}2n\pi N^+-X=\pi, & \text{for } a^+(X),\\ 2n\pi N^--X=-\pi, & \text{for } a^-(X).\end{array} \quad (18)$$

Double wedge structures need to be carefully studied since, as is has been shown by many authors (see, e. g., [9]), the overall diffraction coefficient when both source and observation points are aligned with the common face of the wedge is not the product of two diffraction coefficients (8). Therefore, using expression (18) for the doubly diffracted field by an impedance double wedge given by Herman and Volakis [10] (the reader is referred to that paper for an explanation of all the terms used), it is possible to write:

$$u_{21}^d(\phi_2,\phi_0)=D^{II}(\phi_2,\phi_0,n,m,w,k)\frac{\exp(-jkw)}{\sqrt{w}}\frac{\exp-jk\rho}{\sqrt{\rho}} \quad (19)$$

where the authors have used the following definition for the double diffraction coefficient:

$$D^{II} = \frac{-j}{\pi k (mn)^2} \frac{\Psi(\frac{n\pi}{2}+\pi)\Psi(\frac{m\pi}{2}+\pi)}{\Psi(\frac{n\pi}{2}-\phi_0)\Psi(\frac{m\pi}{2}-\phi_2)} a_1 a_2 a_3 [A\{1-F_{KP}(kwa_1)\} + B\{1-F_{KP}(kwa_2)\} + C\{1-F_{KP}(kwa_3)\}] \cdot \left\{ \frac{1}{1-\cos\left(\frac{\pi-\phi_0}{n}\right)} - \frac{1}{1-\cos\left(\frac{\pi+\phi_0}{n}\right)} - \frac{\sin\left(\frac{\phi_0}{n}\right) C_{on}(0)}{\cos\left(\frac{\pi}{n}\right)-\cos\left(\frac{\phi_0}{n}\right)} \right\} \cdot \left\{ \frac{1}{1-\cos\left(\frac{\pi+\phi_2}{m}\right)} - \frac{1}{1-\cos\left(\frac{\pi-\phi_2}{m}\right)} + \frac{\sin\left(\frac{\phi_2}{m}\right) C_{om}(0)}{\cos\left(\frac{\pi}{m}\right)-\cos\left(\frac{\phi_2}{m}\right)} \right\} \frac{\exp(-jkx)}{2} \quad (20)$$

In the case of a perfect electrical conductor double wedge, the diffraction coefficient used is, for hard polarization:

$$D_{12}^h = \frac{1}{4\pi jk} \sum_{p,q=1}^{2} \frac{(-1)^{p+q}}{n_1 n_2} \cot\left(\frac{\Phi_1^p}{2n_1}\right) \cot\left(\frac{\Phi_2^q}{2n_2}\right) \tilde{T}(a_p, b_q, w) \quad (21)$$

and for soft polarization:

$$D_{12}^h = \frac{-1}{16\pi k^2 l} \sum_{p,q=1}^{2} \frac{(-1)^{p+q}}{n_1 n_2} \csc^2\left(\frac{\Phi_1^p}{2n_1}\right) \csc^2\left(\frac{\Phi_2^q}{2n_2}\right) \tilde{\tilde{T}}(a_p, b_q, w) \quad (22)$$

for the meaning of the various symbols, the reader is referred to [11], [12].

VI. Computation of the field strength

The field strength at the observation point is computed as coherent superposition of all the electromagnetic fields associated with each ray trajectory. Therefore,

$$\vec{E}_{\text{tot,obs}} = \sum_{i=1}^{N} \vec{E}_{\text{obs}}^{\,i} \ , \quad (23)$$

where N is the number of ray trajectories and the field strength of each trajectory is given by:

$$\vec{E}_{\text{obs}}^{\,i} = \vec{E}_{\text{source}} \left(\prod_{k=1}^{K_i} A_k^i \right) \left(\prod_{l=1}^{L_i} R_l^i \right) \times \left(\prod_{m=1}^{M_i} D_m^{i\text{I}} \right) \left(\prod_{n=1}^{N_i} D_n^{i\text{II}} \right) \ . \quad (24)$$

In the previous equation, the symbols used are:

- K_i, the number of free space propagation paths for the i-th trajectory and A_k^i, the attenuation factor;
- L_i, the number of reflections for the i-th trajectory and R_l^i, the reflection coefficient at each location;
- M_i, the number of first-order diffractions along the i-th trajectory and D_m^{II}, the first order diffraction coefficient at each location;
- N_i, the number of second-order diffractions along the i-th trajectory and $D_n^{i\text{II}}$, the second order diffraction coefficient at each location.

VII. Conclusions

Results were not yet available at the time of submission of this manuscript. However, they will be presented at the conference. With this paper the authors have given a contribution towards a systematic approach for the study of electromagnetic scattering by multiple bodies using ray tracing methods. The ideas introduced with this method only require the knowledge of visibility. The same ideas can be extended to three dimensions with the only difference that the numerical routines will have to account for one more dimension. Therefore, with this paper, a three dimensional method has also been implicitly stated.

References

[1] T. Whitthed. An improved illumination model for shaded display. *Commun. ACM*, 23(6):343–349, Jun 1990.

[2] J. Arvo and D. Kirk. A survey of ray tracing acceleration techniques. In Andrew S. Glassner, editor, *An introduction to ray tracing*. Academic Press, 1989.

[3] N. P. Wilt. *Object Oriented Ray Tracing in C++*. Wiley, 1994.

[4] J. Goldsmith and J. Salmon. Automatic creation of object hierarchies for ray tracing. *IEEE Comput. Graph. Appl.*, 7(5):14–20, May 1987.

[5] R. Tiberio, G. Pelosi, and G. Manara. A uniform GTD formulation for the diffraction by a wedge with impedance faces. *IEEE Trans. Antennas Propagat.*, 33(8):867–873, Aug 1985.

[6] T. B. A. Senior and J. L. Volakis. *Approximate boundary conditions in electromagnetics*. IEE, London, UK, 1995.

[7] R. G. Kouyoumjian and P. H. Pathak. A uniform geometrical theory of diffraction for an edge in a perfectly conducting surface. *Proc. IEEE*, 62(11):1448–1461, Nov 1974.

[8] G. D. Maliuzhinets. Excitation, reflection and emission of surface waves from a wedge with given face impedances. In *Sov. Phys. Dokl.*, volume 3, pages 752–755, 1958.

[9] S. -W. Lee, Y. Rahmat-Samii, and R. C. Menendez. GTD, ray field and comments on two papers. *IEEE Trans. Antennas Propagat.*, 26(2):352–354, Mar 1978.

[10] M. I. Herman and J. L. Volakis. High frequency scattering by a double impedance wedge. *IEEE Trans. Antennas Propagat.*, 36(5):664–678, May 1988.

[11] M. Albani, F. Capolino, S. Maci, and R. Tiberio. Diffraction at a thick screen including corrugations on the top face. *IEEE Trans. Antennas Propagat.*, 45(2):277–283, Feb 1997.

[12] F. Capolino, M. Albani, S. Maci, and R. Tiberio. Double diffraction at a pair of coplanar skew edges. *IEEE Trans. Antennas Propagat.*, 45(8):1219–1226, Aug 1997.